# Calculation of a Mass-Consistent Two-Dimensional Wind Field with Divergence Control

MAURIZIO BROCCHINI

*School of Mathematics, University of Bristol, Bristol, United Kingdom and Department of Atmospheric Sciences, University of California, Los Angeles, Los Angeles, California*

MORTON WURTELE

*Department of Atmospheric Sciences, University of California, Los Angeles, Los Angeles, California*

GEORG UMGIESSER AND STEFANO ZECCHETTO

*Istituto Studio Dinamica Grandi Masse, C.N.R., Venice, Italy*

(Manuscript received 25 April 1994, in final form 21 March 1995)

ABSTRACT

The aim of this paper is the calculation of mass-consistent wind velocity field in a two-dimensional domain $\Omega$ on the basis of sparse measurements collected by wind-measuring stations. Measured data are used to estimate an initial field. The result is obtained by a weighted interpolation method. An iterative scan procedure is used in which the radius of influence of each station over the surrounding grid points is decreased at each step of iteration. To adjust the initial field into a mass-consistent velocity wind field, a new technique is presented that is meant to extract only the purely divergent component of the wind velocity field. This component is then either suitably manipulated, reduced and reintroduced in the total wind field, or completely neglected. The main idea of the method is to obtain a mass-consistent wind by controlling the magnitude of the purely divergent component without completely destroying all the information connected with its spatial pattern. On the basis of a test case, the quality of the proposed method is assessed, and a good agreement with observations is found.

## 1. Introduction

Since the first attempt at numerical weather prediction by Richardson (1922), in which the raw divergence of the observed wind field was vertically integrated to produce a forecast pressure change of 125 mb in 6 h, it has been realized that some technique must be adopted to control this most sensitive derived field from observed wind data.

This is equally true on the cyclonic scale and on the mesoscale. When the wind field is to be used directly, and no dynamical modeling is involved, this difficulty is at its most acute because the network grid distance is so comparatively small. An error of 1 m $s^{-1}$ in wind observations separated by 20 km will result in a rate of increase in the height of a 1-km inversion of 360 m per hour. This is not to say that the divergence is zero or even small: on this scale, flow divergence does exist and in fact approaches the vorticity in magnitude.

On the other hand there exists a need of mass-consistent wind velocity fields among the meteorological fields for the initialization of numerical models. This need is well reflected in the large literature (Liu and Goodin 1976; Dickerson 1978; Sherman 1978; Goodin et al. 1979; Moussiopoulos and Flassak 1986; Ludwig et al. 1991) devoted to the analysis of methods for obtaining mass-conserving wind fields. Most of this literature is devoted to large-scale initialization for NWP or a GCM, but the mesoscale surface wind field has also received a share of attention (Ku and Rao 1987; Lu and Turco 1994). These models along with transport and diffusion models are often based on a presumption of mass-conserving flows (Ku and Rao 1987).

A velocity wind field characterized by excessively divergent (or convergent) flows might be a misleading input both for dynamic models and for models used in the air quality management activities.

The problem may be stated as follows: any numerical interpolation of the usually sparsely observed winds to a network of grid points will result in a field with kinematic properties that render it unsuitable for the purposes for which it is intended. In particular, the interpolated wind fields will in general have an associated divergence that is both unrealistically large in magnitude and variable on the scale of the grid itself.

*Corresponding author address:* Maurizio Brocchini, School of Mathematics, University of Bristol, University Walk, Bristol BS8 1TW, United Kingdom.
E-mail: m.brocchini@bristol.ac.uk

If such a wind field is used in computing the dispersion of pollutants, or in ocean wave forecast models, the results will exhibit similar distortions of scale and magnitude. What is desired, therefore, is a means of manipulating the two-dimensional wind field, already interpolated to a grid, in such a way as to control its kinematic properties.

To achieve the intended goal, the sparse input velocity wind measurements are interpolated over the grid by means of a weighting procedure (Goodin et al. 1979; Ku and Rao 1987). A decreasing scan radius is defined to evaluate the weighting function in such a way that the small-scale motions are not transmitted all over the domain $\Omega$ but dominate only within an influence area around each station.

A new method is proposed in this paper and is based on the position that when a relatively high-quality observed wind field is available, there is some information contained in its divergence pattern, and although the magnitude thereof must be controlled, the gross features of the pattern should be preserved.

To achieve this, the method adopted to minimize the divergence of the wind field cannot be based on a purely numerical technique, that is, one that essentially moves the divergence around (see Liu and Goodin 1976), but must retain the spatial characteristics of the initial divergence field.

The fundamental idea is that the wind field is a linear superposition of components: rotation, divergence, and deformation. At first the divergent wind component is isolated from the others by solving the Poisson equation where the divergence itself acts as the source for the field. Then the purely divergent (convergent) component is either manipulated in order to reduce its magnitude and reinserted in the total wind field or subtracted from the total field.

The method proposed herein is specific to produce a smooth field of divergence not to exceed some specified maximum value, but it could also be applied to control vorticity or deformation if this were needed. The particular maximum divergence value specified will depend on the use to be made of the data; for purpose of this work, it is arbitrary.

The material that follows is presented according to a simple scheme. In the second section, the procedure to obtain an initial interpolated wind field from sparse measures is considered. The proposed new method for minimizing the divergent wind field is analyzed in section 3. Sections 4 and 5 summarize, respectively, the results of the chosen test for validating the procedure and an application of the method to a project of environmental management that is currently carried out in Venice, Italy. Finally, some conclusions are given in section 6.

## 2. The initial field

The generation of a continuous wind field from discrete datasets is achieved by a two-step procedure. The first step is the interpolation of the raw station data to a finer mesh that covers the area of interest. The interpolated wind field is then used as an initial guess to the objective analysis procedure, which applies physical constraints (minimum field divergence in out case) to adjust the wind vectors at each grid point.

A procedure is considered based on the hypothesis that the values of the variables at each grid point are weighted averages of the surrounding data. Therefore, if $\mathbf{u} = (u, v)$ is the two-dimensional wind velocity vector, its value at each grid point is computed according to

$$\mathbf{u}_{ij} = \frac{\sum_{k=1}^{N} \mathbf{u}_k W_k(r)}{\sum_{k=1}^{N} W_k(r)}, \tag{1}$$

where $\mathbf{u}_k$ is the value measured at the $k$th station, $W_k(r)$ is the weighting function, $r$ the distance from the considered point $(i, j)$ to the station, and $N$ the number of stations. Cressman (1959) suggested the following weighting factor to be adopted:

$$W(r) = \frac{R^2 - r^2}{R^2 + r^2}, \tag{2}$$

where $R$ is the radius of influence of every station on the surrounding grid points. It represents the distance at which the weighting function $W_k(r) = 0$. Every grid point $(i, j)$ is then influenced by the stations located at distances $r < R$.

This procedure is based on a series of successive scans of the entire domain $\Omega$ with decreasing values of $R$ (called the scan radius) at each scan. Some improvements to the interpolation procedure have been introduced with respect to Cressman's original method.

The first one is related to the scan radius $R$, which can be used either as a fixed value for each iteration over the whole grid or as a variable quantity for each grid point. When using a fixed radius of influence, $R$ is decreased at a fixed rate from a maximum value that is comparable to the typical length scale of the area of interest to a minimum value. For the minimum scan radius, the estimate $R = 1.6(A/N)^{1/2}$ is adopted, where $A$ represents the total area of the region of interest and $N$ the number of measuring stations available in that area (Stephens and Stitt 1970). This relationship was derived after a number of attempts to optimize $R$. On the other hand, when a variable scan radius is adopted, $R$ is decreased at each iteration in such a way that a fixed minimum number of stations will be contained in the influence area of each grid point. The advantage of this latest strategy is that the effects of small-scale motions are confined to the influence area of each grid point with dependence on the local station density. The choice between fixed or variable radius depends

on the density and spatial distribution of measuring stations within each considered domain.

A second change has been introduced in the weighting factor, which has been chosen to be

$$W^k_{i,j}(r^k_{i,j}) = \begin{cases} \left(\dfrac{R^2 - r^{k2}_{i,j}}{R^2 + r^{k2}_{i,j}}\right)^2, & r^k_{i,j} \leq R \\ 0, \quad r^k_{i,j} > R, \end{cases} \tag{3}$$

where $r^k_{i,j}$ is the distance from the grid point $(i, j)$ to the station $k$. This is a function that decreases more rapidly with increasing distance than that used by Cressman. Therefore, the influence of each station on the interpolated wind field is more localized. For a more detailed analysis concerning these arguments the correspondence between Glahn (1981) and Goodin et al. (1981) is a good reference.

The initial field is chosen to be $\mathbf{u} = \mathbf{0}$ except, of course, at the stations. At each step of iteration $m$ the value of the field at each grid point depends on the weighting $W^k_{i,j}$ and on the correction $d\mathbf{u}^m_k$ defined at the $m$th iteration for the $k$th station. The value of the correction factor is obtained by subtracting the observed value at the $k$th station $\mathbf{u}_k$ from the value that the same station had the previous iteration step $\mathbf{u}^{m-1}_k$, that is,

$$d\mathbf{u}^m_k = \mathbf{u}^{m-1}_k - \mathbf{u}_k. \tag{4}$$

Then the error is redistributed over all the domain $\Omega$ weighting it for each grid point

$$\mathbf{u}^{m+1}_{i,j} = \mathbf{u}^m_{i,j} + \frac{\sum_{k=1}^{N} W^k_{i,j} d\mathbf{u}^m_k}{\sum_{k=1}^{N} W^k_{i,j}}, \tag{5}$$

where the weight $W^k_{i,j}$ is evaluated using the grid points falling within the circle of radius $R$. This procedure is run until the percentual error $\epsilon$ at the $m$th iteration is less than a chosen value (10%–15%), where the percentual error is given by

$$\epsilon = \frac{\sum_{k=1}^{N} |d\mathbf{u}^m_k|}{\sum_{k=1}^{N} |\mathbf{u}^m_k|}. \tag{6}$$

## 3. The spurious divergence method

The methodology under investigation (SD method hereafter) allows the definition of a wind field where the "spurious divergence" is reduced to a minimum assigned value. The spurious divergence is the field divergence component artificially introduced by the interpolation of sparse data on a regular grid. In the following, the considered problem is described and the method is explained, this involves both the analysis of the chosen boundary conditions and the analysis of the numerical methodology adopted.

### *a. The problem and the method*

It may be instructive to consider the general problem of the kinematic manipulation of a two-dimensional vector field. We know that such a field consists of divergence, vorticity, and deformation—the latter being so-called shearing and stretching fields, which are related by a simple rotation of the coordinate axis. Let us say that we wish first to identify and then to control the magnitude of each of these quantities. Is this possible? Is it even a well-posed problem?

The mathematical theorems necessary to answer these questions are recorded in any treatment of kinematics or potential theory (e.g., Batchelor 1967, chapter 2). We represent the two-dimensional vector field as decomposed into vorticity, divergence, and deformation, respectively, by

$$\mathbf{u} = \mathbf{u}_r + \mathbf{u}_d + \mathbf{u}_f. \tag{7}$$

Given an observed wind field, how may these three components thereof be determined? We know that nondivergent vector fields and irrotational vector fields may be expressed in terms of scalar quantities. Thus,

$$\mathbf{k} \cdot \nabla \times \mathbf{u}_r = \nabla^2 \psi = \zeta(x, y) \tag{8}$$

$$\nabla \cdot \mathbf{u}_d = \nabla^2 \phi = D(x, y) \tag{9}$$

$$\mathbf{k} \cdot \nabla \times \mathbf{u}_f = \nabla \cdot \mathbf{u}_f = \nabla^2 \chi = 0. \tag{10}$$

So stated, this is a complex boundary value problem (Batchelor 1967, 84–108). We can in principle apply two different methods to (9) to recover this component field of the observed field from which the divergence $D$ is calculated. They are, respectively, based on the technique of Green's function applied to the above-mentioned equations and the direct solution of the equation by Poisson solvers. The rotational field (8) we can solve for with certain assumptions about the boundary values. These may be considered particular solutions. In the case of the deformation (10), we require the homogeneous solution: a vector field that has neither divergence nor curl. Here, theory tells us that the field is determined solely by its boundary values. These are not known as separate from those of the other components, but the field can perhaps be determined as a residue when the other two have been calculated. It is not necessary to write explicitly the integral solution to this problem since this is not the method pursued in the present article. The point is that some assumptions or approximations must be incorporated in any solution procedure to the total problem. A systematic treatment of this total problem would be useful. However, we consider in this paper the control of only one of these components, the divergent velocity field.

We choose to use the fast procedure guaranteed by Poisson solvers to separate the purely divergent field $\mathbf{u}_d$ from the other components. In principle this component can be either minimized at wish or completely eliminated from the original interpolated wind field to obtain a final mass-conserving flow field.

*b. The boundary conditions*

Since we choose a direct method of solution of (9), we now address the question of the boundary conditions for the potential function $\phi$. We will consider boundary conditions leading to minimum kinetic energy of the divergent flow (see Pedersen 1971).

By using an obvious extension of Pedersen's argument to the present problem, we conclude that the boundary condition that minimizes the divergent kinetic energy is

$$\phi = 0 \tag{11}$$

on $\partial\Omega$.

*c. The numerical procedure*

As already mentioned, the total field is separated into two main components: the purely divergent component $\mathbf{u}_d$ and a residual component combining the rotational, shearing, and stretching contributions:

$$\mathbf{u}_{\text{tot}} = \mathbf{u}_d + \mathbf{u}_{\text{res}}. \tag{12}$$

Thus, the whole numerical procedure can be subdivided as a sequence involving the following four steps:

1) Evaluation of the initial field divergence (coming from the interpolation iterative procedure) by means of a scheme of second-order accuracy, that is,

$$D_{i,j} = \frac{u_{i+1,j} - u_{i-1,j}}{2\Delta x} + \frac{v_{i,j+1} - v_{i,j-1}}{2\Delta y}. \tag{13}$$

2) Solution of the Poisson equation $\nabla^2\phi = D(x, y)$, with boundary condition $\phi = 0$ on $\partial\Omega$. Poisson's equation is thus written according to the following finite-difference scheme:

$$D_{i,j} = \frac{\phi_{i+1,j} - 2\phi_{i,j} + \phi_{i-1,j}}{(\Delta x)^2} + \frac{\phi_{i,j+1} - 2\phi_{i,j} + \phi_{i,j-1}}{(\Delta y)^2}. \tag{14}$$

Equation (14) is solved by a successive overrelaxation procedure where the potential function is stepped according to the following weighted average:

$$\phi_{i,j}^{m+1} = \omega\phi_{i,j}^{*m} + (1 - \omega)\phi_{i,j}^{m}; \tag{15}$$

$\omega$ being the overrelaxation parameter and

$$\phi_{i,j}^{*m} = \frac{(\Delta y)^2(\phi_{i+1,j}^{m} + \phi_{i-1,j}^{m}) + (\Delta x)^2 \times (\phi_{i,j+1}^{m} + \phi_{i,j-1}^{m}) - D_{i,j}(\Delta x)^2(\Delta y)^2}{2[(\Delta x)^2 + (\Delta y)^2]}. \tag{16}$$

The method is convergent for $0 < \omega < 2$, and the optimal choice for $\omega$ is given by

$$\omega = \frac{2}{1 + (1 - \rho_{\text{Jac}}^2)^{1/2}}, \tag{17}$$

where the Jacobi radius of convergence for a rectangular $I \times J$ grid is

$$\rho_{\text{Jac}} = \frac{\cos(\pi/I) + (\Delta x/\Delta y)^2 \cos(\pi/J)}{1 + (\Delta x/\Delta y)^2}. \tag{18}$$

The number of iterations $n$ to reduce the overall error by a factor $10^{-s}$ is therefore estimated:

$$n \approx \frac{sI \ln 10}{2\pi} \approx \frac{1}{3} sI, \tag{19}$$

showing that the asymptotic rate of convergence depends linearly on both the required accuracy $s$ and the size of the analyzed domain $I$. However, this asymptotic convergence rate is not attained until of order $I$ iterations, but at that stage usually the error has grown by about one order of magnitude. A simple modification of the scheme is obtained allowing for a variable relaxation parameter, which is time stepped according to the recurrence relation of Chebyshev polynomials (Golub and Varga 1961). Since the optimum asymptotic relaxation parameter $\omega$ is not necessarily a good initial choice, $\omega$ is changed at each step according to the following rule:

$$\omega_{(1)} = 1; \quad \omega_{(2)} = \frac{2}{(2 - \rho_{\text{Jac}}^2)^2};$$

$$\omega_{(m+1)} = \frac{4}{[4 - \rho_{\text{Jac}}^2\omega_{(m)}]}, \quad m = 2, 3, \cdots \tag{20}$$

optimizing both the initial and the asymptotic value for $\omega$ itself. However, it is well known that the convergence of this iterative procedure is rather slow for large numbers of grid points. Therefore, a more suitable algorithm when dealing with a large number of grid points should be based on multigrid techniques.

3) Computation of the divergent wind field component $\mathbf{u}_d$ is performed according to

$$\mathbf{u}_d = \nabla\phi. \tag{21}$$

4) Subtraction of the divergent component from the total wind field $\mathbf{u}_{\text{tot}}$:

$$\mathbf{u}_{\text{res}} = \mathbf{u}_{\text{tot}} - \mathbf{u}_{\text{d}}. \tag{22}$$

Theoretically at this stage the residual component should contain no divergence at all. On the other hand, we have experience that running the procedure just once decreases the initial divergence by about one order of magnitude all over the domain $\Omega$, reaching a maximum divergence of about $10^{-5}$ s$^{-1}$ at each grid point. This value represents the upper acceptable limit for the

natural divergence, usually found within the atmospheric boundary layer. The reason for this persistance of divergence after applying the procedure is related to the boundary conditions. In fact it is evident that most of the residual divergence is found at the boundary of the domain. However, in order to improve the result and reach a final divergence of $O(10^{-6}\ s^{-1})$ or even less, the above-mentioned procedure can be iterated. Iterating the procedure reduces the divergence at the boundaries and, consequently, all over the domain.

## 4. Test results

To verify the performance of both the interpolating procedure and of the SD method, a test case has been set up in which meteorological data relative to the "Los Angeles basin," have been used. This has been made possible by the availability at the University of California, Los Angeles, of a set of 24 graphic maps representing wind speed measures averaged over 24 years (1950–73) for each month of the year. The 24 daily measures (one each hour) were collected by 60 stations within the Los Angeles basin and interpolated by Keith and Selik (1977). The maps give both the average wind values at the stations and the interpolation of the values by streamlines. The whole procedure (interpolation and SD method) has been tested against the wind field of September and comparison with given streamlines has been tried. The month of September has been chosen since the streamlines coming from Keith and Selik were accurately checked and improved by J. G. Edinger (1978, personal communication).

Even if this sort of comparison may seem subjective, it gives a good description of the quality of the reproduced field. However, it must be coupled with the analysis of the final vector field and with an error analysis between interpolated and final field to definitively assess the validity of the method. Thus, for the SD method a more quantitative analysis has been performed based on the percentual error of the modulus of the final wind field with respect to the modulus of the interpolated one. On the other hand, it has to be pointed out that no objective comparison can be done between the initial wind field (available only in sparse locations) and the final one since it would make no sense to obtain a good agreement on the station locations if the field at large was wrong.

Figure 1 shows the distribution of the measuring stations with the domain $\Omega$ used for the simulations. This is a rectangular mesh of $51 \times 35$ squares with a grid size of 2514 m. The left and the top boundaries of the domain will be referred to, respectively, as the geographical west and north.

Only two particular cases among those available have been chosen as typical situations occurring in the Los Angeles basin. They are relative to hours 0000 and 1500 Pacific standard time (PST). The first case (0000 PST) is a typical situation where the wind field is not driven by sea-breeze phenomena and a marked directional pattern is not present. The winds are relatively weak, and the topography can generate small local vorticity effects. On the other hand, in the 1500 PST case there is a moderate sea breeze blowing from southwest to east. The wind pattern is almost uniform all over the domain $\Omega$.

In Figs. 2 and 3 are shown the measured sparse data field and the interpolated field, respectively, for each of the two situations. In these two cases the model gives a good interpolation of the sparse data field. Computation was stopped when the total percentual error defined in section 2 was of $\epsilon = 10\%$ for the 1500 PST case, while for the case 0000 PST the error could not be decreased under $\epsilon = 20\%$. In both cases, however, the differences between the maximum wind values were sufficiently small: 3.0 m $s^{-1}$ for the given field and 3.5 m $s^{-1}$ for the interpolated one at 0000 PST; 7.5 m $s^{-1}$ for the given field and 8.4 m $s^{-1}$ for the interpolated one at 1500 PST.

We now analyze, in more detail, the performance of the SD method.

### *a. The 0000 PST case*

The first comparison to be considered is between the initial divergence field and the final one, that is, after removing the purely divergent wind component by means of the SD method (see Fig. 4). Maximum values of initial divergence are of about $1 \times 10^{-4}\ s^{-1}$ in the south region of the considered domain (Santa Ana area: SNA) and in the area centered on the station UCLA. On the contrary, minimum values of the same order of magnitude are found in the east region of Pomona (POM) and above San Pedro Promontory (see stations TIH and HBR). The final divergence field is characterized by maximum and minimum values of one order of magnitude smaller. It is evident that the method adopted "smooths" the initial field and consequently adjusts the velocity wind field, but it also retains many characteristics of the positive–negative divergence field pattern. Excess of divergence is forced to move toward the closest boundaries of the domain without any preferred direction.

Figure 5 shows the streamlines of the wind field taken from Keith and Selik (1977) and revised at UCLA by J. G. Edinger and those coming from the SD technique. The two streamlines patterns are in good agreement, though the Edinger's field better represents the small local features. In fact the main features of the field are properly reproduced, for example, the two regions of flow rotation centered on the LAX and POM stations, respectively.

Comparison of the vector plots of the interpolated and final wind velocity field (Fig. 5) reveals that most of the changes to the interpolated wind field due to the

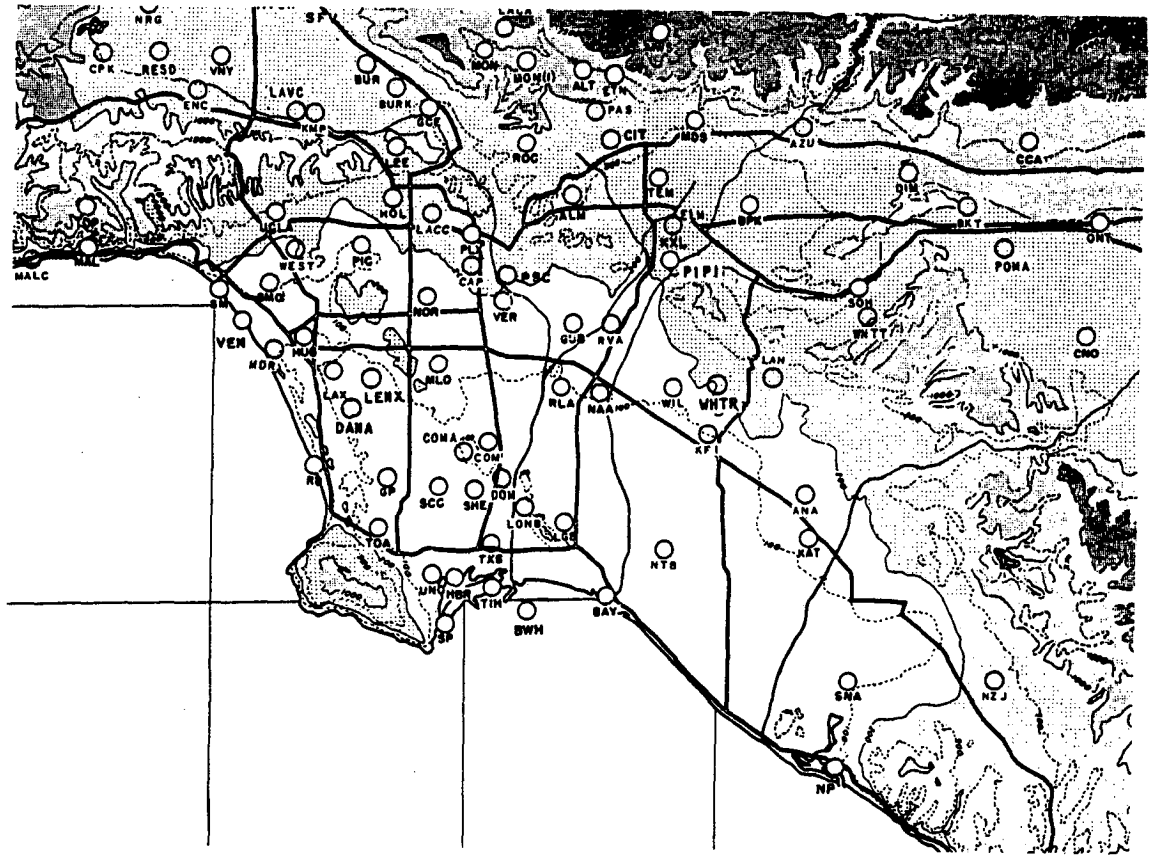


FIG. 1. Locations of observation sites and terrain contour, and the domain adopted for the simulations in the Los Angeles basin.

action of the SD procedure occurs in the northeast region of the domain, in the area centered on the POM station, and in the region of San Pedro Promontory (see stations TIH and HBR). This is an expected result, as we have previously seen that those areas are characterized by the highest initial divergence values. The final wind field maximum values are of about 3.0 m $s^{-1}$, which compare well with both the interpolated

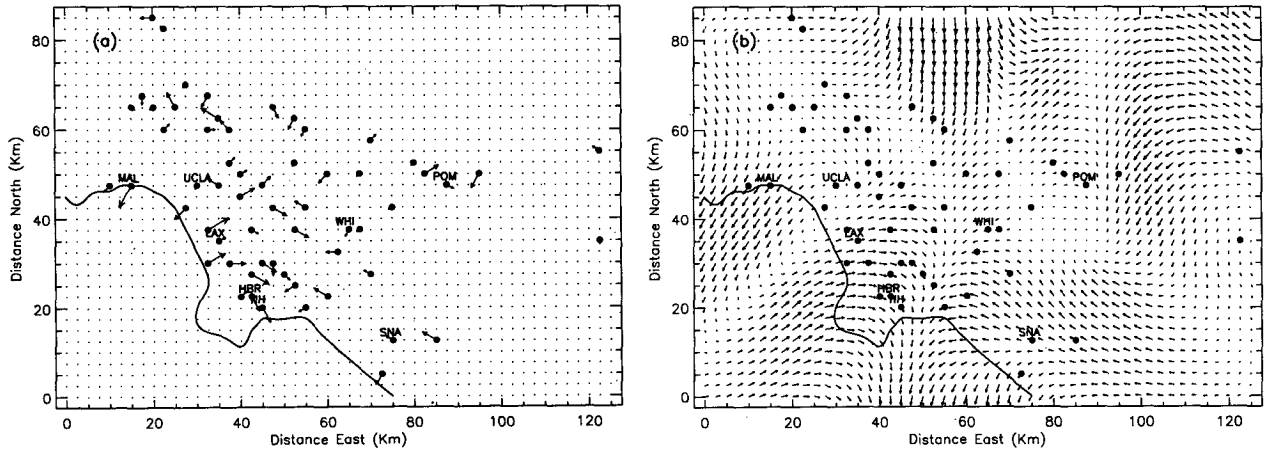


FIG. 2. Wind analysis for 0000 PST (September): (a) the measured data field and (b) the interpolated velocity wind field. The maximum wind speeds are measured 3.0 m $s^{-1}$, interpolated 3.5 m $s^{-1}$.

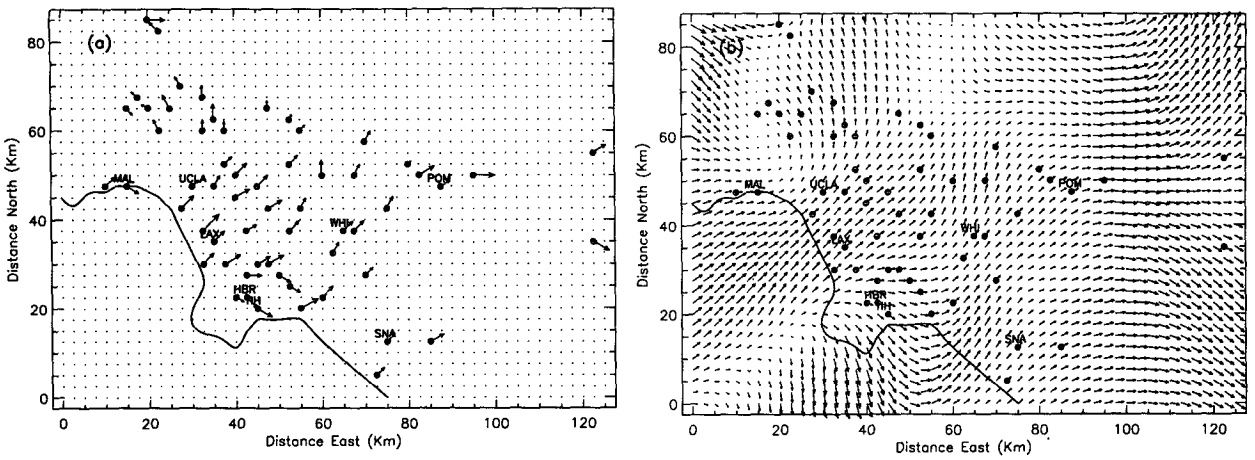


FIG. 3. Wind analysis for 1500 PST (September): (a) the measured data field and (b) the interpolated velocity wind field. The maximum wind speeds are measured 7.5 m $s^{-1}$, interpolated 8.4 m $s^{-1}$.

value 3.5 m $s^{-1}$ and the initial maximum value of 3.0 m $s^{-1}$ (Fig. 6).

A final comparison is given by analyzing the contour plots of the difference between vector magnitude of the interpolated and final field (Fig. 10). In most of the domain the difference between the two fields is less than 40%. However, there are a few regions where this difference reaches up to 80%, and they are again regions where most of the changes of the wind divergence occur.

### *b. The 1500 PST case*

The same sort of comparisons of the case 0000 PST are carried out. In this case, maximum values of initial divergence are larger than for the previous case (see Fig. 7) and are of about $5 \times 10^{-4}$ $s^{-1}$ in the south region of the considered domain (San Pedro Promontory), in an area north of the station UCLA, and in the area centered on the POM station. Minimum values of the same order of magnitude are found in the northwest corner of the domain and in an area north of the station WHI. Again the final divergence field is characterized by maximum and minimum values of one order of magnitude smaller. And again the excess of divergence is forced to move toward the closest boundaries of the domain where maximum values of divergence are found $3 \times 10^{-5}$ $s^{-1}$.

Figure 8 shows the streamlines comparison against Edinger's streamlines. The comparison in this case is even better than for the 0000 PST case. In fact now the wind pattern is strongly dominated by the breeze pattern, which generates an almost uniform offshore–inland direction for the flow. Moreover, the wind ro-

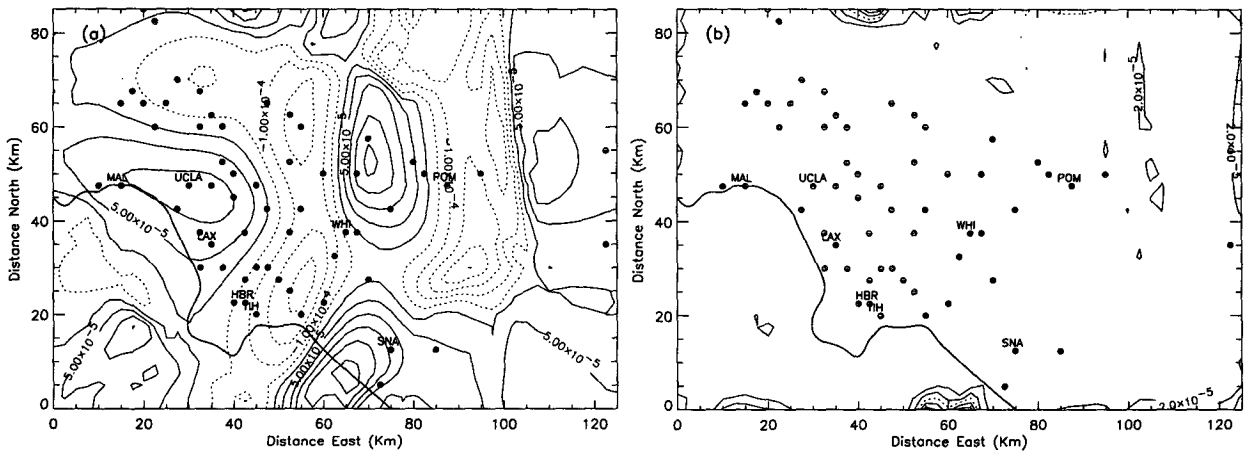


FIG. 4. Divergence field analysis for 0000 PST (September): (a) initial divergence field and (b) final divergence field. Solid lines and broken lines are used, respectively, for positive and negative contour values.

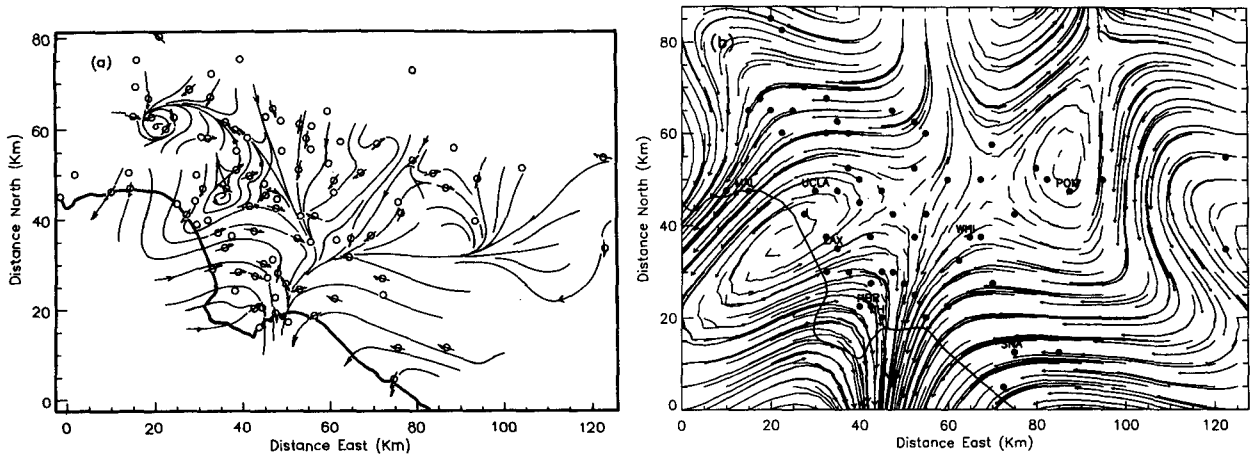


FIG. 5. Wind fields comparison. Final field at 0000 PST: (a) streamlines from the interpolation by J. G. Edinger and (b) streamlines from the proposed SD technique.

tation occurring north of MAL is well represented by the computed streamlines.

Comparison of the vector plots of the interpolated and final wind velocity field (Fig. 8) shows that the major effects of the use of the SD method are felt in the region of the San Pedro Promontory (stations TIH and HBR), where the strong inland–offshore flow field is transformed into a weaker rotational pattern. Maximum wind velocity is of about 8.1 m $s^{-1}$ against the 7.5 and 8.4 m $s^{-1}$ values of the initial and interpolated fields, respectively (Fig. 9).

However, the best comparison is given in this case by the contour plots of the relative error between vector magnitude of the interpolated and final field (Fig. 10). Regions where the difference exceeds a value of 40% are a very small fraction of the whole domain and are located at the northwest corner of the domain.

## 5. The Venice Lagoon case

We now apply the already described method to the analysis of the wind fields above the Venice Lagoon. The importance of this sort of analysis is both in defining proper wind fields for air quality management and in initializing the numerical hydrodynamic models applied to the internal circulation of the lagoon itself. The water circulation inside the lagoon has been studied so far as essentially triggered by the water levels at the lagoon mouths. These depend on the Adriatic Sea astronomical and meteorological tides, as well as the second-order effects produced by the atmospheric pressure and the wave setup. The effect of storm surge induced by the wind blowing directly over the lagoon is known, but its study has been almost neglected in the past, apart from the works of Dazzi et al. (1987)

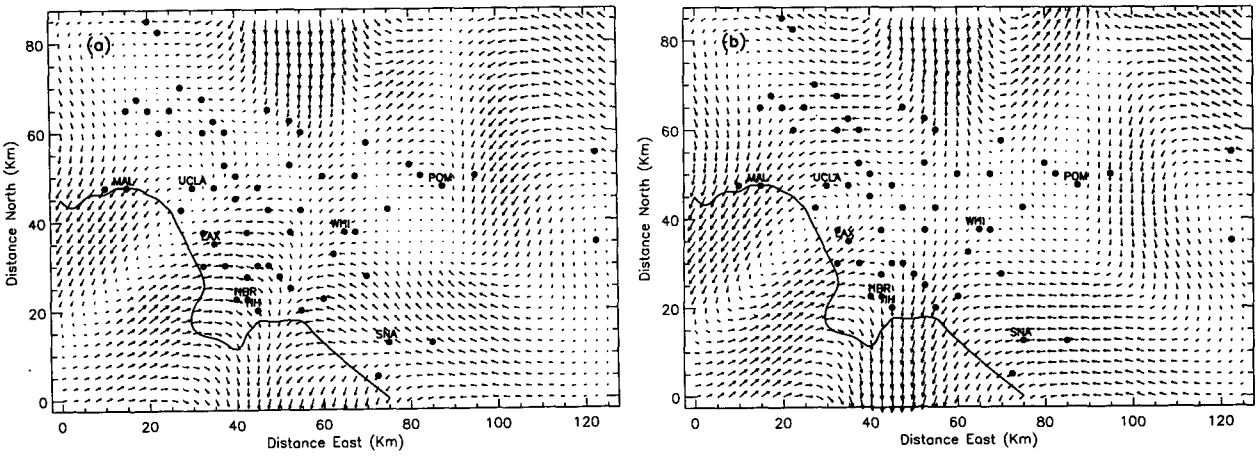


FIG. 6. Wind field comparison. Final field at 0000 PST: (a) vector representation for the interpolated field and (b) vector representation for the proposed SD technique. The maximum wind speed is 3.5 m $s^{-1}$ for the interpolated field and 3.0 m $s^{-1}$ for the SD technique.

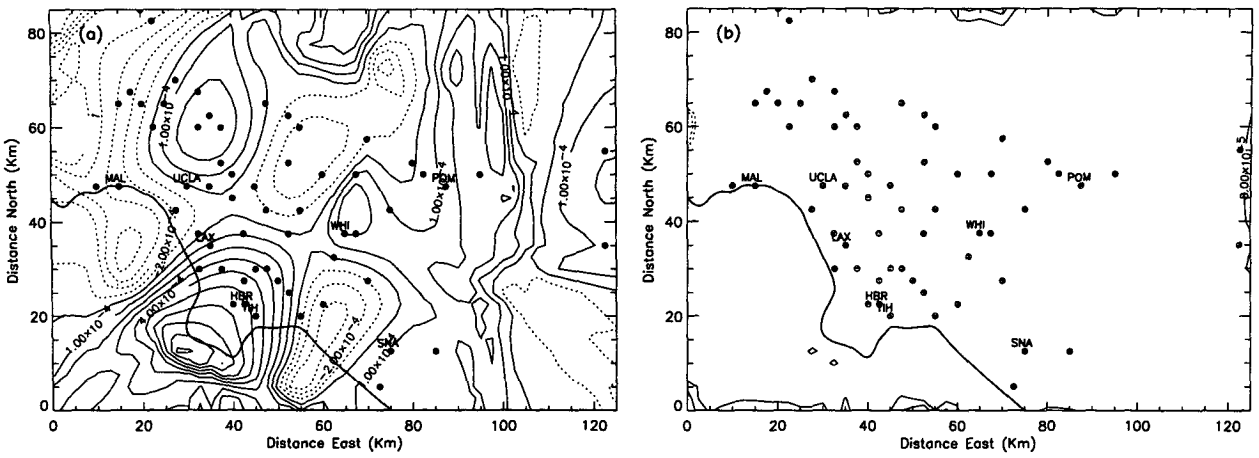


FIG. 7. Divergence field analysis for 1500 PST (September): (a) initial divergence field and (b) final divergence field. Solid lines and broken lines are used, respectively, for positive and negative contour values.

and Pirazzoli (1981). It goes without saying that the precise determination of the wind field over the lagoon is of chief importance in this context. For this aim, a network of five stations measuring the wind field has been recently set up in the Venice Lagoon. This allows simultaneous collection of wind data, which is then transmitted in quasi-real time to the Istituto per lo Studio della Dinamica delle Grandi Masse (I.S.D.G.M.) where the data analysis takes place. The study of the storm surge inside the lagoon is carried out using a hydrodynamic model that requires a wind field input over a regular grid. The necessity of an interpolation scheme to transform the measured winds into a regular spaced wind field is one of the primary reasons for developing the present objective analysis methodology.

Unfortunately, only four of the five mentioned stations are operational at present, and a sample of data collected on the 21 October 1994 is analyzed. It refers to the data sample obtained at 1800 hours.

In Fig. 11a the adopted geometry for the Venice Lagoon is shown with the locations of the four considered stations (PETTA, VAL, S.GIO, and TES). The region southeast of the lagoon boundary represents the Adriatic Sea, while northwest of the lagoon we find the inland Venetian area. Three large isles are present within the lagoon, the northernmost of which represents the area where most of the city of Venice is built.

This dataset is mainly intended to show how the SD method works rather than being used as a comparison case. We also consider here a situation in which the method is used iteratively rather than in a single computation step.

The initial field (maximum velocity of 12.7 m $s^{-1}$) has been interpolated, and the interpolation procedure

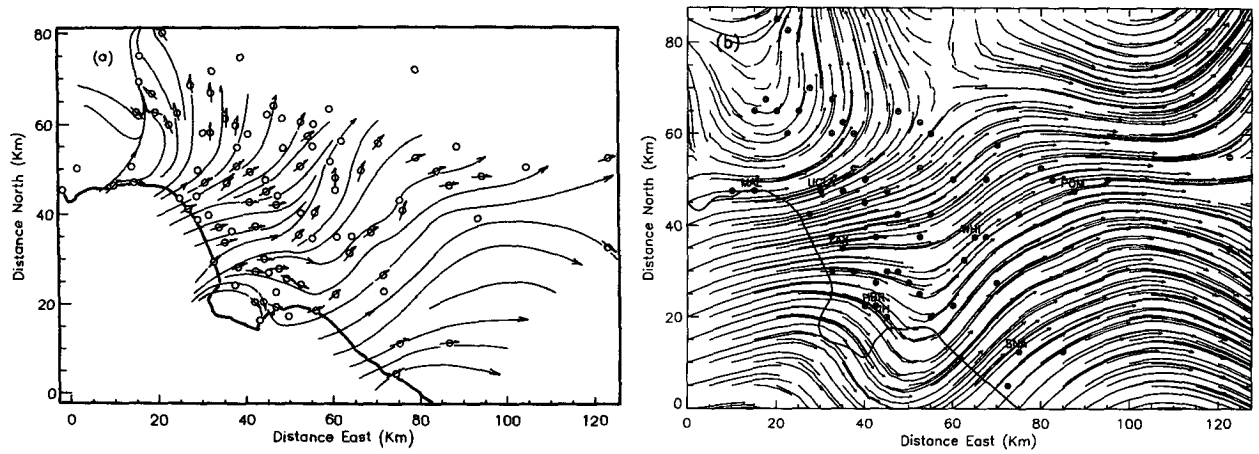


FIG. 8. Wind fields comparison. Final field at 1500 PST: (a) streamlines from the interpolation by J. G. Edinger and (b) streamlines from the proposed SD technique.

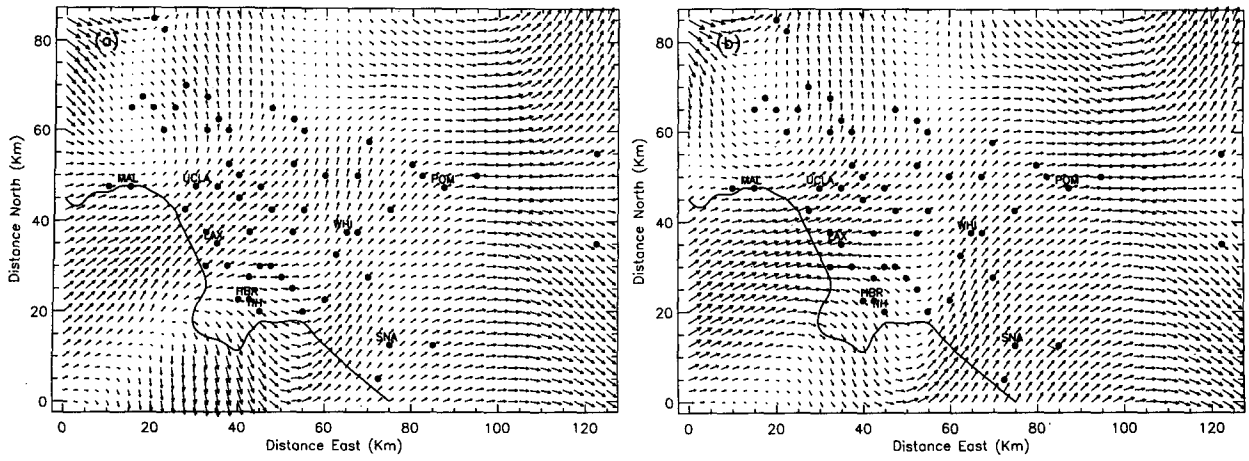


FIG. 9. Wind fields comparison. Final field at 1500 PST: (a) vector representation for the interpolated field and (b) vector representation for the proposed SD technique. The maximum wind speed is 8.4 m $s^{-1}$ for the interpolated field and 8.1 m $s^{-1}$ for the SD technique.

has been stopped when the relative error reached a value of $\epsilon = 2\%$. The good accuracy obtained for this test is basically related to the little number of available data; that is, the redistribution of wind errors at the stations is only forced by four constraints. In other words, the good accuracy only states that the available data have been properly used to build the interpolated wind field; however, this does not guarantee that a locally physically sensible wind field has been obtained because of the coarse coverage of the area by measured winds. The final wind field is characterized by a maximum velocity value of about 13.7 m $s^{-1}$ (see Fig. 11b).

We now concentrate our attention to the extraction of the purely divergent wind field from the total wind. In Fig. 12, the purely divergent component is shown at two different iterations of the SD method. The initial divergent field has a magnitude of about 5 m $s^{-1}$ while the same component is reduced, after 10 iterations of the SD method, to a value of about 0.2 m $s^{-1}$.

As a consequence of that, the divergence itself is reduced as seen in Fig. 13. The initial divergence contours are characterized by a maximum value of about $2 \times 10^{-3}$ $s^{-1}$. Contour plots of the divergence after 1 and 10 iterations show that divergence has been decreased by one and two orders of magnitude, respectively. It is, however, significant that the maximum and minimum of divergence are still found at the same location where the initial ones were placed.

## 6. Conclusions

An accurate procedure and methodology to interpolate sparse data onto a regular grid has been achieved. A new technique to determine a diver-

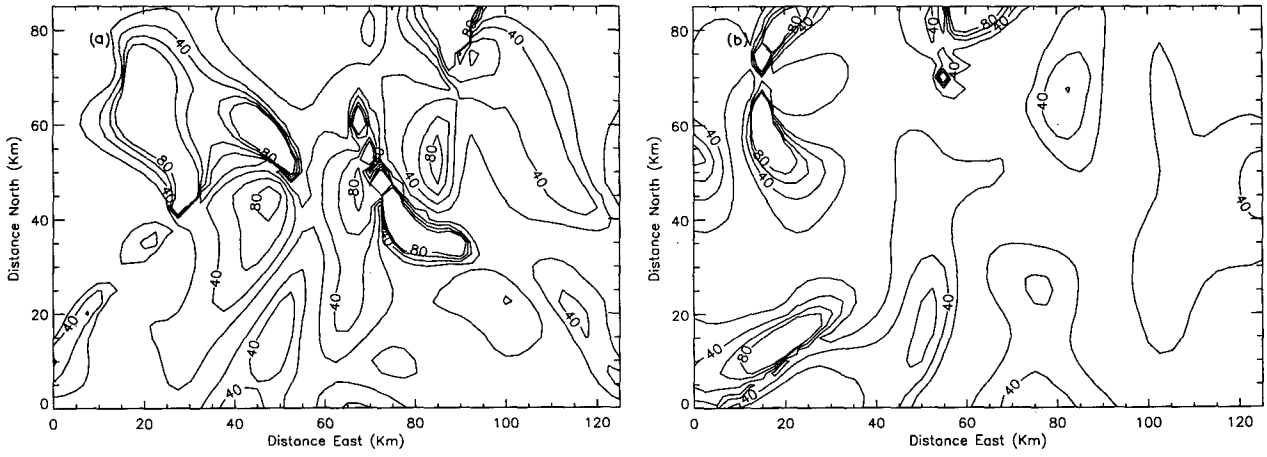


FIG. 10. Contour plots of the percentual error between modulus of the interpolated wind field and modulus of the final wind field: (a) 0000 PST and (b) 1500 PST.

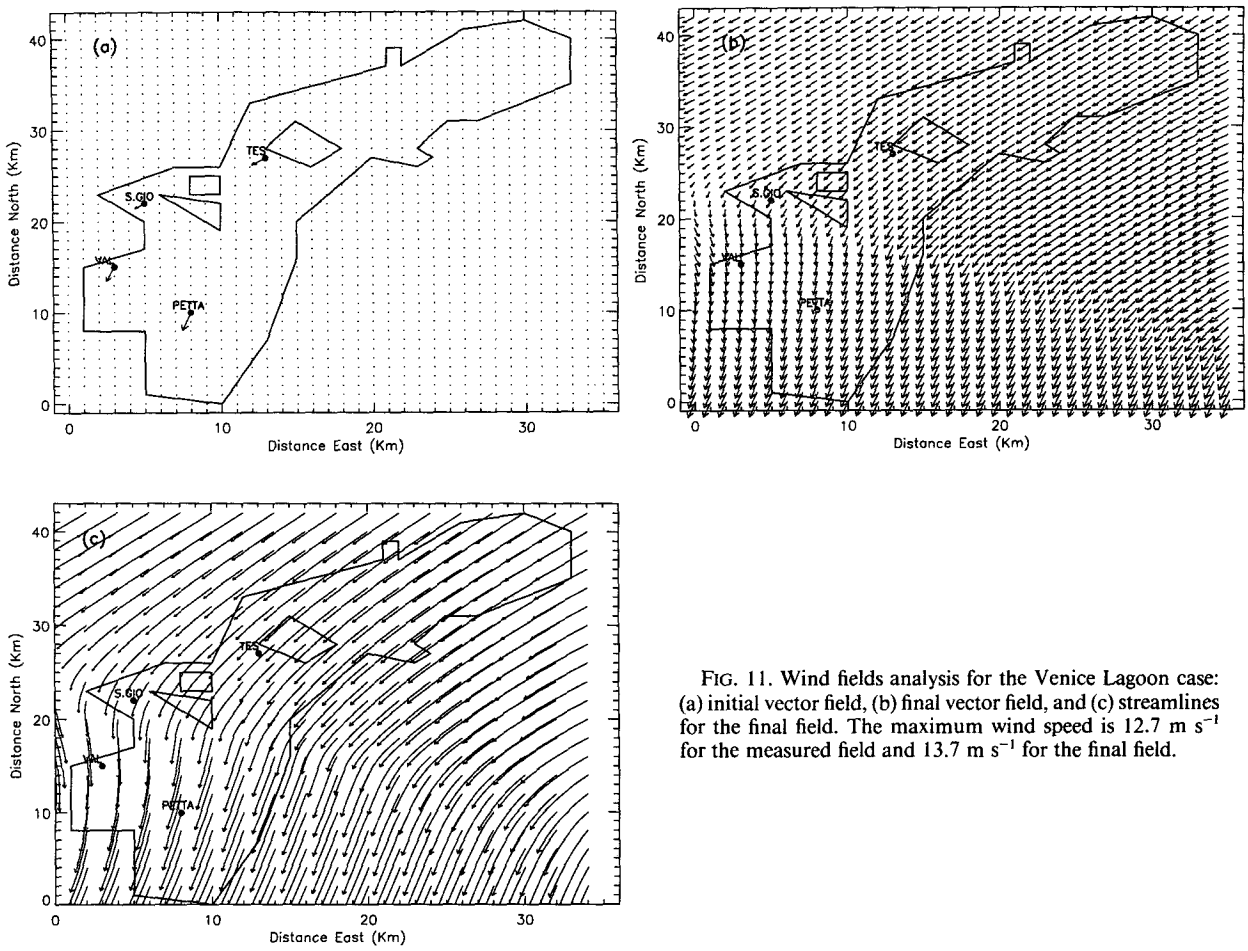


FIG. 11. Wind fields analysis for the Venice Lagoon case: (a) initial vector field, (b) final vector field, and (c) streamlines for the final field. The maximum wind speed is 12.7 m $s^{-1}$ for the measured field and 13.7 m $s^{-1}$ for the final field.

gence-free two-dimensional field has been analyzed. The proposed technique ["spurious divergence" minimization (SD)] is based on the view that when a relatively high-quality observed wind field is available, there is some information contained in its divergence pattern, and although the magnitude

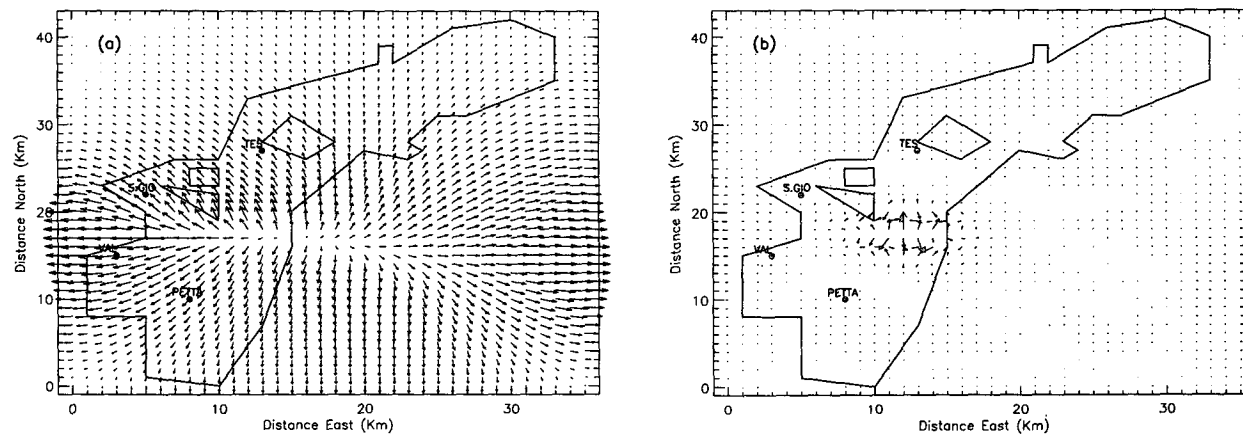


FIG. 12. Wind fields analysis for the Venice Lagoon case: (a) initial divergent vector field and (b) divergent vector field after 10 iterations of the SD technique. The maximum wind speed is 5.0 m $s^{-1}$ for the initial divergent field and 0.2 m $s^{-1}$ for the final one.

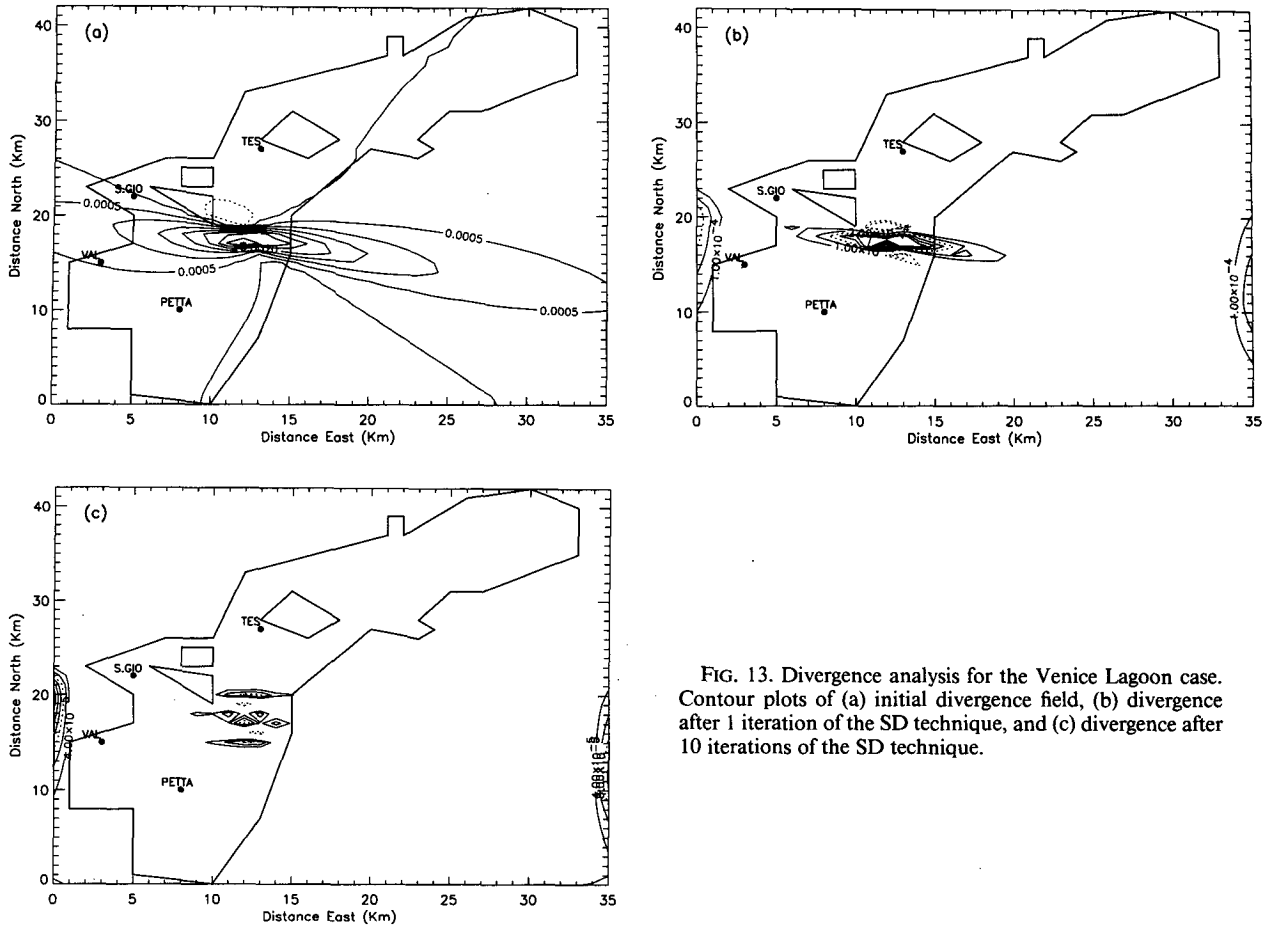


FIG. 13. Divergence analysis for the Venice Lagoon case. Contour plots of (a) initial divergence field, (b) divergence after 1 iteration of the SD technique, and (c) divergence after 10 iterations of the SD technique.

thereof must be controlled, the pattern should be preserved. The purely divergent wind component is therefore extracted from the total wind field, which can be separated into three main contributions: rotational, divergent, and deformation components. The procedure allows for a reduction of one order of magnitude of the initial divergence. Iterating the procedure can reduce the initial divergence up to 100 times. However, the initial divergence cannot be decreased to any required level.

The results obtained by this method show that both the flow pattern and the magnitude of the highest wind values can be well reproduced even when the input sparse data field is characterized by strong gradients.

A possible improvement to the SD method can be introduced if the purely divergent wind component is extracted by means of the Green's function technique applied to the Poisson equation where the field divergence acts as the source. This would in fact overcome the problem presented by a residual divergence at the boundary, which characterizes the direct solution of Poisson's equation.

*Acknowledgments.* This work has been funded by the Italian Ministery of Science and Technology (MURST) under the project "Sistema Lagunare Veneziano."

The authors thank Dr. Robert Sharman and Dr. Celal S. Konor for the very useful discussions.

## REFERENCES

Batchelor, G. K., 1967: *An Introduction to Fluid Dynamics.* Cambridge University Press, 615 pp.

Cressman, G. P., 1959: An operational objective analysis system. *Mon. Wea. Rev.*, **87**, 367–374.

Dazzi, R., G. Rossi, A. Rusconi, and A. Tomasin, 1987: *Meteorologia e laguna:* L'ammonimento delle piu' recenti bufere per l'efficacia degli interventi di difesa. Istituto Veneto di Scienze Lettere ed Arti, Vol. X, Comm. Studio Provv. Con. Dif. laguna e citta' di Venezia.

Dickerson, M. H., 1978: MASCON—A mass consistent atmospheric flux model for regions with complex terrain. *J. Appl. Meteor.*, **17**, 241–253.

Glahn, H. R., 1981: Comments on "A comparison of interpolation methods for sparse data: Application to wind and concentration fields." *J. Appl. Meteor.*, **20**, 88–91.

Golub, G. H., and R. S. Varga, 1961: Chebyshev semi-iterative methods, successive overrelaxation iterative methods, and second order Richardson methods. Part I. *Num. Math.*, **3**, 147–156.

Goodin, W. R., G. J. McRae, and J. H. Seinfield, 1979: A comparison of interpolation methods for sparse data: Application to wind and concentration fields. *J. Appl. Meteor.*, **18,** 761–771.

——, ——, and ——, 1981: Reply. *J. Appl. Meteor.*, **20,** 92–94.

Keith, R. W., and B. Selik, 1977: California south coast air basin hourly wind flow patterns. Air programs Division Report. South Coast Air Quality Management District Headquarters, 288 pp.

Ku, J. Y., and S. T. Rao, 1987: Numerical simulation of air pollution in urban areas: Model development. *Atmos. Environ.*, **21,** 201–212.

Liu, C. Y., and W. R. Goodin, 1976: An iterative algorithm for objective wind field analysis. *Mon. Wea. Rev.*, **104,** 784–792.

Lu, R., and R. P. Turco, 1994: Air pollutant transport in a coastal environment. Part I: Two-dimensional simulations of sea-breeze and mountain effects. *J. Atmos. Sci.*, **51,** 2285–2308.

Ludwig, F. L., J. M. Livingstone, and R. M. Endlich, 1991: Use of mass conservation and critical dividing streamline concepts for efficient objective analysis of winds in complex terrain. *J. Appl. Meteor.*, **30,** 1490–1499.

Moussiopoulos, N., and T. Flassak, 1986: Two vectorized algorithms for the effective calculation of mass-consistent flow fields. *J. Appl. Meteor.*, **25,** 847–857.

Pedersen, K., 1971: Balanced systems of equations for the atmospheric motion. *Geofys. Publ.*, **28,** 1–12.

Pirazzoli, P. A., 1981: Bora e acqua alta. *Acqua-Aria,* **10.**

Richardson, 1922: *Weather Prediction by Numerical Process.* Cambridge University Press.

Shermann, C. A., 1978: A mass-consistent model for wind fields over complex terrain. *J. Appl. Meteor.*, **17,** 312–319.

Stephens, J. J., and J. M. Stitt, 1970: Optimum influence radii for interpolation with the method of successive corrections. *Mon. Wea. Rev.*, **98,** 680–687.